Revista de la Academia Colombiana de Ciencias Exactas, Físicas y Naturales. 2026
doi: https://doi.org/10.18257/raccefyn.3606

Chemical Sciences

Original article

Second-order many-body perturbation theory for the any particle molecular orbital method in the framework of Hartree products of localized wave functions

Teoría de perturbaciones de muchos cuerpos de segundo orden para el método de orbitales moleculares de cualquier partícula cuántica en el marco de productos de Hartree de funciones de onda localizadas

Andrés Reyes

Departamento de Química, Universidad Nacional de Colombia - sede Bogotá, Colombia

Inaugural article as Corresponding Member of the Academia Colombiana de Ciencias Exactas, Físicas y Naturales

Abstract

This paper presents an alternative second-order many-body perturbation theory (MBPT(2)) for the Any Particle Molecular Orbital (APMO) method. Here, the reference wave function was constructed as a product of Slater determinants for light species (e.g., electrons) and Hartree products of localized orbitals for heavy species (e.g., muons, nuclei). The impact of this Hartree product approximation (HPA) on APMO/MBPT(2) energies was analyzed for the hydrogen molecule and hydrogen-bonded dimers. It was observed that the impact of the HPA on the first-order energies is negligible. In contrast, the HPA-induced changes in the nuclear-electron correlation terms led to reductions of the order of 10^{-2} a.u. in the second-order energies. APMO/MBPT(2)/HPA energies are closer to the full-CI energies than APMO/MBPT(2) energies. The Hartree product approximation (HPA) for heavy particles modifies virtual orbital energies, leading to increased correlation recovery similar to improved virtual orbital techniques in post-Hartree-Fock methods. Specifically, the HPA reduces virtual nuclear orbital energies, resulting in smaller energy denominators in the perturbation expansion and, thus, larger interspecies correlation corrections. However, the amount of interspecies correlation recovered is limited and system-dependent. The application to systems containing multiple hydrogen nuclei revealed that the HPA leads to reductions in the formal scaling of nuclear-electron and nuclear-nuclear integral transformations from quintic to quartic and cubic, respectively. These reductions allow APMO/MBPT(2) calculations for much larger systems. The application of the APMO/MBPT(2) method to muonic helium and lithium atoms and the muonic helium dimer revealed that the muon-electron correlation is of the order of only 1×10^{-6} a.u. This work provides a methodological and computational contribution, offering a pragmatic, low-cost approximation for exploratory studies of nuclear quantum effects in medium-sized systems. The primary advantage is the reduction in computational scaling, enabling exploration of larger systems and potential energy surfaces.

Keywords: Any particle molecular orbital; many-body perturbation theory; nuclear quantum effects; muonic Chemistry; LOWDIN code.

Resumen

Se presenta una teoría alternativa de perturbaciones de muchos cuerpos de segundo orden (MBPT(2)) para el método de orbitales moleculares para cualquier partícula (*Any-Particle Molecular Orbital*, APMO). En dicho marco, la función de onda de referencia se construyó como un producto de determinantes de Slater para especies ligeras (por ejemplo, electrones) y productos de Hartree de orbitales localizados para especies pesadas (por ejemplo, muones y núcleos). Se analizó el impacto de esta aproximación de producto de Hartree (*Hartree Product Approximation*, HPA) en las energías APMO/MBPT(2) en la molécula de hidrogeno y en dímeros unidos por enlaces de hidrogeno. Se observó que el efecto de la HPA en las energías de primer orden es despreciable. En cambio, la HPA introduce cambios en los términos de correlación núcleo-electrón, lo que conduce a reducciones del

Citation: Reyes A. Second-order many-body perturbation theory for the any particle molecular orbital method in the framework of Hartree products of localized wave functions. Revista de la Academia Colombiana de Ciencias Exactas, Físicas y Naturales. 2026 Sep 21. doi: https://doi.org/10.18257/raccefyn.3606

Editor: Luis Fernando Echeverri

***Corresponding author:**
Andrés Reyes; areyesv@unal.edu.co

Received: November 27, 2025
Accepted: June 25, 2026
Published on line: September 21, 2026

Revista de la Academia Colombiana de Ciencias Exactas, Físicas y Naturales. 2026
doi: https://doi.org/10.18257/raccefyn.3606

orden de 10^{-2} u.a. en las energías de segundo orden. Las energías APMO/MBPT(2)/HPA están más cercanas a las energías de interacción de configuración completa (*full-CI*) que las energías APMO/MBPT(2) convencionales. La aplicación a sistemas que contienen múltiples núcleos de hidrógeno reveló que la HPA reduce el escalado formal de la transformación de integrales núcleo-electrón y núcleo-núcleo, pasando de quintico a cuártico y cúbico, respectivamente. Estas reducciones permiten realizar cálculos APMO/MBPT(2) en sistemas mucho más grandes. La aplicación del método APMO/MBPT(2) a átomos de helio y litio muónicos, así como al dímero de helio muónico, muestra que la correlación muón-electrón es del orden de apenas 1×10^{-6} u.a. Este trabajo constituye una contribución metodológica y computacional que ofrece una aproximación pragmática y de bajo costo para estudios exploratorios de efectos cuánticos nucleares en sistemas de tamaño medio. La principal ventaja reside en la reducción de la complejidad computacional, lo que permite explorar sistemas más grandes y superficies de energía potencial.

Palabras clave: orbitales moleculares para cualquier partícula; teoría de perturbaciones de muchos cuerpos; efectos cuánticos nucleares; química muónica; programa LOWDIN.

1 Introduction

The Born–Oppenheimer approximation (Born & Oppenheimer, 1927) (BOA) is a cornerstone of molecular physics and chemistry. It underpins a broad range of applications—from spectroscopy to quantum chemistry—and enables the treatment of molecular systems with thousands of electrons and nuclei (Peng et al., 2008).

Although quantum chemistry techniques grounded in the Born–Oppenheimer approximation (BOA) are highly successful, they neglect nuclear quantum effects (NQE) on the electronic structure because the BOA strictly separates electronic and nuclear motions. For many molecular systems, these NQEs are negligible, but in systems with light or strongly delocalized nuclei, they can become pronounced (Ishimoto et al., 2009; Nakai, 2007; Udagawa & Tachikawa, 2009).

Over the past few decades, various methodologies have been developed to go beyond the BOA and incorporate NQE explicitly into electronic structure and molecular geometry calculations. These include the Nuclear Orbital plus Molecular Orbital (NOMO) method (Nakai, 2002; Tachikawa et al., 1998), the Multi-Component Molecular Orbital (MCMO) method (Tachikawa, 2002), the Nuclear-Electronic Orbital (NEO) approach (Webb et al., 2002), and the Any Particle Molecular Orbital (APMO) approach (González et al., 2008; Reyes et al., 2019). A key advantage of these nuclear molecular orbital (NMO) techniques is that NQEs on electronic structure and molecular properties are obtained within a single computation, rather than being introduced as subsequent corrections.

Within the NMO Hartree–Fock (HF) approach, the total wave function is expressed as a direct product of electronic and nuclear components, represented by Slater determinants for fermions and symmetric products for bosons. The corresponding Hartree–Fock–Roothaan equations for both electrons and nuclei are solved in a fully coupled manner. Beyond HF, the NMO formalism has been generalized to more advanced electronic-structure treatments, such as second-order Møller–Plesset perturbation theory (MBPT(2)) (González & Reyes, 2010; Hoshino & Nakai, 2006; Ishimoto et al., 2006; Nakai & Sodeyama, 2003; Swalina et al., 2005), configuration interaction and multiconfigurational approaches (Charry et al., 2018; Ishimoto, Tachikawa, & Nagashima, 2008; Nakai & Sodeyama, 2003; Tachikawa, 2002; Tachikawa & Osamura, 2000; Webb et al., 2002), coupled-cluster theory (Fowler & Brorsen, 2022; Nakai & Sodeyama, 2003; Pavošević et al., 2019), and explicitly correlated wave function methods (Charry Martinez et al., 2022; Hoshino et al., 2011; Stanke et al., 2026), among others.

NMO approaches employing HF-based electronic and nuclear wave functions have been effectively applied to explore NQEs in a broad range of molecular systems. These include studies of diatomic-molecule anharmonicity (Hoshino et al., 2007), primary and secondary

isotope effects on molecular structure and stability (González & Reyes, 2010; González et al., 2008; Kaneko et al., 2010; Moncada, Uribe, et al., 2013a; Moreno et al., 2010; Nakai et al., 2007; Tanaka et al., 2025; Udagawa & Tachikawa, 2006; Udagawa et al., 2006), kinetic isotope effects (Ishimoto, Ishihara, et al., 2008; Kikuta et al., 2008), ionization energies (Pedraza-González et al., 2016; Romero et al., 2012), phase transitions in ferroelectrics (Ishii et al., 2025; Moncada et al., 2010; Tachikawa, 2008; Tachikawa et al., 2002), and NQEs on magnetic properties (Kita & Tachikawa, 2009), among others. In several cases, explicitly accounting for electron–nuclear correlation substantially refines stabilization energies and equilibrium internuclear distances (González & Reyes, 2010; Moncada, Uribe, et al., 2013b; Moreno et al., 2010), and, in extreme situations, produces dramatic symmetry changes in low-barrier hydrogen-bonded systems (Moreno et al., 2011; Yodsin et al., 2025).

Previous work has shown that NMO/HF computations can be made substantially more efficient by expressing the proton wave function as a Hartree product of localized proton orbitals instead of a Slater determinant.(Auer & Hammes-Schiffer, 2010; Nakai, 2002) These studies further demonstrated that the nuclear Hartree product approximation (HPA) has a negligible effect on the NMO/HF energy, owing to the strong localization of the nuclear orbitals and the negligible magnitude (on the order of 10^{-10} a.u. (Nakai, 2002; Reyes et al., 2005)) of the nuclear exchange term omitted in the HPA. Nakai and Sodeyama (2003) also introduced an independent particle model (IPM), which is equivalent to the nuclear HPA, for use in many-body perturbation theory and coupled-cluster NMO methods. However, they did not present the explicit theoretical formulation of the IPM or assess its quantitative effect on total energies.

Our group has introduced the APMO methodology (Reyes et al., 2019), a generalization of the NMO formalism applicable to arbitrary quantum particles. We have previously employed APMO at the HF level to investigate nuclear quantum effects in molecules (González et al., 2008) and to analyze atoms incorporating negative muons (Moncada, Cruz, & Reyes, 2013a; Moncada et al., 2012; Posada et al., 2014). Although the Hartree product approximation (HPA) for heavy particles has been utilized in related multicomponent approaches, this study presents the first systematic derivation, implementation, and numerical investigation of MBPT(2) within the APMO/HPA framework. Our focus is chiefly on methodological and computational aspects, but we also examine the impact of the HPA on MBPT(2) interspecies correlation energies.

Recent advances in explicitly correlated multicomponent techniques, coupled-cluster schemes for multicomponent systems, and other correlation approaches deliver very high accuracy at the expense of increased computational cost, whereas the method introduced here serves as a low-cost alternative suitable for exploratory studies.

In the following, APMO/HF and APMO/HF/HPA denote the standard APMO HF method and its variant incorporating HPA, respectively. The corresponding second-order MBPT methods are labeled APMO/MBPT(2) and APMO/MBPT(2)/HPA.

The paper is organized as follows. Section 2 reviews the APMO/HF, APMO/HF/HPA, APMO/MBPT(2), and APMO/MBPT(2)/HPA methods. Section 3 addresses computational aspects. In section 4, the APMO/MBPT(2)/HPA scheme is applied to model systems to evaluate its numerical performance and efficiency. Section 5 presents concluding remarks.

2 Theory

We begin by outlining the general any-particle electronic wave function and energy formulations used in the APMO/HF (González et al., 2008; Nakai, 2002; Tachikawa et al., 1998), APMO/MBPT(2) (González & Reyes, 2010; Ishimoto et al., 2006; Swalina et al., 2005), and APMO/HF/HPA approaches. On this foundation, we formulate the working equations

Revista de la Academia Colombiana de Ciencias Exactas, Físicas y Naturales. 2026
doi: https://doi.org/10.18257/raccefyn.3606

for the APMO/MBPT(2)/HPA approach.

2.1 APMO/HF theory

In this approach (González et al., 2008), the molecular system comprises N_C classical nuclei and N_Q quantum particles. For clarity, we restrict the quantum particles to fermions. The system Hamiltonian is then expressed in terms of kinetic and potential energy operators:

$$H_{tot} = -\sum_{i}^{N_Q} \frac{1}{2M_i}\nabla_i^2 + \sum_{i}^{N_Q}\sum_{j>i}^{N_Q} \frac{q_i q_j}{r_{ij}} + \sum_{i}^{N_Q}\sum_{J}^{N_C} \frac{q_i q_J}{r_{iJ}} + \sum_{I}^{N_C}\sum_{J>I}^{N_C} \frac{q_I q_J}{r_{IJ}}. \tag{1}$$

At this level, the molecular wave function Ψ_0 is represented as a product of single-configuration wave functions Φ_α associated with the various quantum species α.

$$\Psi_0 = \prod_{\alpha}^{N_{types}} \Phi_\alpha, \tag{2}$$

Here, each Φ_α is represented by a Slater determinant of molecular orbitals (MOs) $\psi_{\alpha i}$. N_{types} is the number of types of quantum species.

APMO/HF equations are written in terms of effective one-particle operators for quantum species, α

$$f_\alpha(i)\psi_{\alpha i} = \varepsilon_{\alpha i}\psi_{\alpha i}, \;\; i = 1,\ldots,N_\alpha, \;\; \alpha = 1,\ldots,N_{types}, \tag{3}$$

where N_α is the number of particles of α type. Each f_α can be written as

$$f_\alpha(i) = h_\alpha(i) + \sum_{j}^{N_\alpha} q_\alpha^2 [J_{\alpha j} - K_{\alpha j}] + \sum_{\beta\neq\alpha}^{N_{types}}\sum_{j}^{N_\beta} q_\alpha q_\beta J_{\beta j}, \tag{4}$$

here α and β are labels for the different quantum species. $h_\alpha(i)$ is the core Hamiltonian for one particle,

$$h_\alpha(i) = -\frac{\nabla_i^2}{2M_\alpha} + \sum_{J}^{N_C} \frac{q_\alpha q_J}{r_{iJ}} \tag{5}$$

and J_α and K_α are Coulomb and exchange operators,

$$J_{\alpha j}(1)\psi_{\alpha i}(1) = \left[\int d\mathbf{r}_2 \psi_{\alpha j}^*(2)\frac{1}{r_{12}}\psi_{\alpha j}(2)\right]\psi_{\alpha i}(1), \tag{6}$$

$$K_{\alpha j}(1)\psi_{\alpha i}(1) = \left[\int d\mathbf{r}_2 \psi_{\alpha j}^*(2)\frac{1}{r_{12}}\psi_{\alpha i}(2)\right]\psi_{\alpha j}(1). \tag{7}$$

The resulting eigenvalues for occupied orbitals are

$$\varepsilon_{\alpha a} = \langle a_\alpha|h|a_\alpha\rangle + \sum_{b_\alpha}^{N_\alpha} q_\alpha^2 \langle a_\alpha b_\alpha||a_\alpha b_\alpha\rangle + \sum_{\beta}^{N_{types}}\sum_{a_\beta}^{N_\beta} q_\alpha q_\beta \langle a_\alpha a_\beta|a_\alpha a_\beta\rangle, \tag{8}$$

and the eigenvalues for virtual orbitals are

$$\varepsilon_{\alpha r} = \langle r_\alpha|h|r_\alpha\rangle + \sum_{a_\alpha}^{N_\alpha} q_\alpha^2 \langle r_\alpha a_\alpha||r_\alpha a_\alpha\rangle + \sum_{\beta}^{N_{types}}\sum_{a_\beta}^{N_\beta} q_\alpha q_\beta \langle r_\alpha a_\beta|r_\alpha a_\beta\rangle. \tag{9}$$

here $\{a_\alpha,\, b_\alpha\}$ and $\{r_\alpha,\, s_\alpha\}$ are indices for the occupied and virtual molecular orbitals, respectively, of quantum species α.

By solving Eq. 3, one obtains the MOs associated with species α, each expressed as a linear combination of Gaussian-type functions (GTFs). As indicated in Eq. 4, the effective field acting on a given quantum species is determined by the MOs of all other species.

2.2 APMO/MBPT(2) theory

Within this approach (González & Reyes, 2010; Hoshino & Nakai, 2006; Ishimoto et al., 2006; Nakai & Sodeyama, 2003), the Rayleigh–Schrödinger perturbation theory employs the following reference Hamiltonian:

$$H_0 = \sum_{\alpha}^{N_{types}} \sum_{i}^{N_\alpha} \left[h_\alpha(i) + \sum_{j}^{N_\alpha} q_\alpha^2 [J_{\alpha j} - K_{\alpha j}] + \sum_{\beta \neq \alpha}^{N_{types}} \sum_{j}^{N_\beta} q_\alpha q_\beta J_{\beta j} \right]. \tag{10}$$

The fluctuation operator takes the form:

$$W = \sum_{\alpha}^{N_{types}} \sum_{i}^{N_\alpha} \left[\sum_{j>i}^{N_\alpha} \frac{{q_\alpha}^2}{r_{ij}} + \sum_{\beta>\alpha}^{N_{types}} \sum_{j}^{N_\beta} \frac{q_\alpha q_\beta}{r_{ij}} \right] - \sum_{\alpha}^{N_{types}} \sum_{i}^{N_\alpha} \left[\sum_{j}^{N_\alpha} q_\alpha^2 [J_{\alpha j} - K_{\alpha j}] + \sum_{\beta \neq \alpha}^{N_{types}} \sum_{j}^{N_\beta} q_\alpha q_\beta J_{\beta j} \right]. \tag{11}$$

The APMO/HF energy corrected by MBPT(2) is

$$\mathrm{E}_{\mathrm{APMO/MBPT(2)}} = \mathrm{E}_{\mathrm{APMO/HF}} + \sum_{\alpha}^{N_{types}} \mathrm{E}^{(2)}_{\alpha\alpha} + \sum_{\alpha}^{N_{types}} \sum_{\beta>\alpha}^{N_{types}} \mathrm{E}^{(2)}_{\alpha\beta}. \tag{12}$$

The second-order correction to the energy for particles of the same species is

$$\mathrm{E}^{(2)}_{\alpha\alpha} = \frac{q_\alpha^2}{4} \sum_{a_\alpha}^{N_\alpha} \sum_{b_\alpha}^{N_\alpha} \sum_{r_\alpha > N_\alpha}^{B_\alpha} \sum_{s_\alpha > N_\alpha}^{B_\alpha} \frac{| \langle a_\alpha b_\alpha \,||\, r_\alpha s_\alpha \rangle |^2}{\varepsilon_{\alpha a} + \varepsilon_{\alpha b} - \varepsilon_{\alpha r} - \varepsilon_{\alpha s}}, \tag{13}$$

here B_α is the number of basis functions of the α species. $\{a_\alpha, b_\alpha\}$ and $\{r_\alpha, s_\alpha\}$ are indices for the occupied and virtual molecular orbitals, respectively.

The second-order energy correction to the interaction between species of different types is

$$\mathrm{E}^{(2)}_{\alpha\beta} = q_\alpha q_\beta \sum_{a_\alpha}^{N_\alpha} \sum_{a_\beta}^{N_\beta} \sum_{r_\alpha > N_\alpha}^{B_\alpha} \sum_{r_\beta > N_\beta}^{B_\beta} \frac{| \langle a_\alpha a_\beta \mid r_\alpha r_\beta \rangle |^2}{\varepsilon_{\alpha a} + \varepsilon_{\beta a} - \varepsilon_{\alpha r} - \varepsilon_{\beta r}}. \tag{14}$$

2.3 APMO/HF/HPA theory

In this approach, light particles (electrons) are treated separately from heavy particles (such as nuclei or muons). For clarity, we restrict ourselves to two quantum species—electrons and a single type of heavy particle—although the generalization to any number of species is direct. The Hamiltonian of a system with N_e electrons, N_m heavy particles, and N_C point-like charges is

$$\begin{aligned} H_{tot} = &- \sum_{i}^{N_e} \frac{1}{2} \nabla_i^2 + \sum_{i}^{N_e} \sum_{j>i}^{N_e} \frac{1}{r_{ij}} - \sum_{i}^{N_e} \sum_{J}^{N_C} \frac{q_J}{r_{iJ}} - \sum_{m}^{N_m} \frac{1}{2M_m} \nabla_i^2 \\ &+ \sum_{m}^{N_m} \sum_{n>m}^{N_m} \frac{q_m^2}{r_{mn}} + \sum_{i}^{N_m} \sum_{J}^{N_C} \frac{q_m q_J}{r_{mJ}} + \sum_{I}^{N_C} \sum_{J>I}^{N_C} \frac{q_I q_J}{r_{IJ}}. \end{aligned}$$

The electronic wave function, Φ_e, is expressed as a Slater determinant of spin orbitals, while the heavy-particle wave function is given by a Hartree product of localized orbitals, ψ_m:

$$\Psi_0 = \Phi_e \prod_{m}^{N_m} \psi_m, \tag{15}$$

Revista de la Academia Colombiana de Ciencias Exactas, Físicas y Naturales. 2026
doi: https://doi.org/10.18257/raccefyn.3606

here N_n is the number of heavy particles. Each heavy particle is treated as a distinguishable particle. The resulting HF equations are written in terms of effective one-particle operators,

$$f_e(i)\psi_{ei} = \varepsilon_{ei}\psi_{ei}, \qquad i = 1,\ldots,N_e, \tag{16}$$

$$f_m(1)\psi_{m1} = \varepsilon_{m1}\psi_{m1}, \qquad m = 1,\ldots,N_m, \tag{17}$$

where N_e is the number of electrons. Because of the distinguishability of the heavy particles, there is no particle index (i) associated with them.

Fock operators, f_e and f_m, are written as

$$f_e(i) = h_e(i) + \sum_j^{N_e}[J_{ej} - K_{ej}] - \sum_m^{N_m} q_m J_{m1}, \tag{18}$$

$$f_m(1) = h_m(1) + \sum_{m'\neq m}^{N_m} q_m q_{m'} J_{m'1} - \sum_j^{N_e} q_m J_{ej}. \tag{19}$$

Note that Eq. 19 contains no exchange operators K for identical heavy particles. Consequently, the Coulomb sum over J excludes self-interaction terms. The prime on the m' index specifies that the operator $f_m(1)$ accounts only for interactions with heavy particles apart from m.

The resulting eigenvalues for occupied orbitals are

$$\varepsilon_{ea} = \langle a_e|h|a_e\rangle + \sum_{b_e}^{N_e}\langle a_e b_e||a_e b_e\rangle + \sum_m^{N_m} q_m\langle a_e 1_m|a_e 1_m\rangle, \tag{20}$$

$$\varepsilon_{m_1} = \langle 1_m|h|1_m\rangle + \sum_{m'\neq m}^{N_m} q_m q_{m'}\langle 1_m 1_{m'}|1_m 1_{m'}\rangle + \sum_{a_e}^{N_e} q_m\langle 1_m a_e|1_m a_e\rangle, \tag{21}$$

and the eigenvalues for virtual orbitals are

$$\varepsilon_{er} = \langle r_e|h|r_e\rangle + \sum_{a_e}^{N_e}\langle r_e a_e||r_e a_e\rangle + \sum_m^{N_m} q_m\langle r_e 1_m|r_e 1_m\rangle, \tag{22}$$

$$\varepsilon_{mr} = \langle r_m|h|r_m\rangle + \sum_{m'\neq m}^{N_m} q_m q_{m'}\langle r_m 1_{m'}|r_m 1_{m'}\rangle + \sum_{a_e}^{N_e} q_m\langle r_m a_e|r_m a_e\rangle. \tag{23}$$

Electronic and heavy-particle molecular orbitals are expressed as linear combinations of GTFs. Within the HPA, each heavy particle is treated as a distinguishable species and assigned its basis set. Eliminating the non-local exchange terms decouples the heavy-particle equations, thereby simplifying the SCF procedure. In addition, employing a Hartree product reduces the heavy-particle part to the diagonalization of small single-particle matrices. The electronic and heavy-particle MOs are then obtained by iteratively solving Eqs. 16 and 17.

2.4 APMO/MBPT(2)/HPA theory

Within this approach, the Rayleigh–Schrödinger perturbation theory employs the following reference Hamiltonian:

$$H_0 = \sum_i^{N_e}\left[h_e(i) + \sum_j^{N_e}[J_{ej} - K_{ej}] - \sum_m^{N_m} q_m J_{m1}\right] + \sum_m^{N_m}\left[h_m - \sum_j^{N_e} q_m J_{ej} + \sum_{m'\neq m}^{N_m} q_m q_{m'} J_{m'1}\right]. \tag{24}$$

The fluctuation operator takes the following form:

$$W = \sum_{i}^{N_e}\sum_{j>i}^{N_e}\frac{1}{r_{ij}} + \sum_{m}^{N_m}\sum_{m'>m}^{N_m}\frac{q_m q_{m'}}{r_{mm'}} - \sum_{i}^{N_e}\sum_{m}^{N_m}\frac{q_m}{r_{im}} - \sum_{i}^{N_e}\sum_{j}^{N_e}[J_{ej} - K_{ej}] - \sum_{m}^{N_m}\sum_{m'\neq m}^{N_m} q_m q_{m'} J_{m'1} + \sum_{i}^{N_e}\sum_{m}^{N_m} q_m J_{m1} + \sum_{m}^{N_m}\sum_{j}^{N_e} q_m J_{ej}. \quad (25)$$

The APMO/HF/HPA energy corrected by MBPT(2) is as follows:

$$\mathrm{E}_{\mathrm{APMO/MBPT(2)/HPA}} = \mathrm{E}_{\mathrm{APMO/HF/HPA}} + \mathrm{E}^{(2)}_{ee} + \mathrm{E}^{(2)}_{mm'} + \mathrm{E}^{(2)}_{em}, \quad (26)$$

where the electronic second-order energy correction term is

$$\mathrm{E}^{(2)}_{ee} = \frac{1}{4}\sum_{a_e}^{N_e}\sum_{b_e}^{N_e}\sum_{r_e>N_e}^{B_e}\sum_{s_e>N_e}^{B_e}\frac{|\langle a_e b_e \,||\, r_e s_e\rangle|^2}{\varepsilon_{ea} + \varepsilon_{be} - \varepsilon_{er} - \varepsilon_{es}}, \quad (27)$$

the heavy particle second-order energy correction term is

$$\mathrm{E}^{(2)}_{mm'} = \sum_{m}^{N_m}\sum_{m'>m}^{N_m}\sum_{r_m>1}^{B_m}\sum_{r_{m'}>1}^{B_{m'}} q_m q_{m'}\frac{|\langle 1_m 1_{m'} \mid r_m r_{m'}\rangle|^2}{\varepsilon_{m1} + \varepsilon_{m'1} - \varepsilon_{mr} - \varepsilon_{mr}}, \quad (28)$$

and the heavy particle-electron second-order energy correction term is

$$E^{(2)}_{em} = \sum_{m}^{N_m}\sum_{a_e}^{N_e}\sum_{r_m>1}^{B_m}\sum_{r_e>N_e}^{B_e} q_m\frac{|\langle a_e 1_m \mid r_e r_m\rangle|^2}{\varepsilon_{ea} + \varepsilon_{m1} - \varepsilon_{er} - \varepsilon_{mr}}. \quad (29)$$

2.5 Translation- and rotation-free APMO calculations

In APMO treatments where every particle is described as a quantum wave, it is essential to subtract the translational and rotational contributions from the total energy, since the GTF basis functions do not properly represent these types of motion (Nakai et al., 2005). To address this, Nakai and co-workers introduced a modified NOMO Hamiltonian that excludes these degrees of freedom (Nakai et al., 2005). For a system containing electrons and N_m heavy particles (nuclei or muons), the Translation- and Rotation-Free (TRF) Hamiltonian, omitting two-particle terms, is given by (Nakai et al., 2005)

$$H_{\mathrm{TRF}} = H_{\mathrm{tot}} + \frac{1}{2M_{\mathrm{TOT}}}\sum_{m=1}^{N_m}\nabla^2_m - \sum_{m=1}^{N_m}\sum_{\alpha\in\{x,y,z\}}\frac{(L^0_{\alpha m})^2}{2I^0_\alpha} \quad (30)$$

Here, M_{TOT} denotes the total mass of the system, $L^0_{\alpha m}$ the angular momentum operator, and I^0_α the corresponding principal moment of inertia of the rigid rotor. Calculations performed with this Hamiltonian are termed TRF-APMO calculations.

Regardless of the use of the HPA, these corrections modify the core Hamiltonians, h_m, for the heavy particles,

$$h_m(i) = -\left(\frac{1}{M_m} - \frac{1}{M_{TOT}}\right)\frac{\nabla^2_i}{2} - \sum_{\alpha}^{x,y,z}\frac{{L^0_{\alpha i}}^2}{2I^0_\alpha} + \sum_{j}^{N_C}\frac{q_m q_J}{r_{iJ}}. \quad (31)$$

Revista de la Academia Colombiana de Ciencias Exactas, Físicas y Naturales. 2026
doi: https://doi.org/10.18257/raccefyn.3606

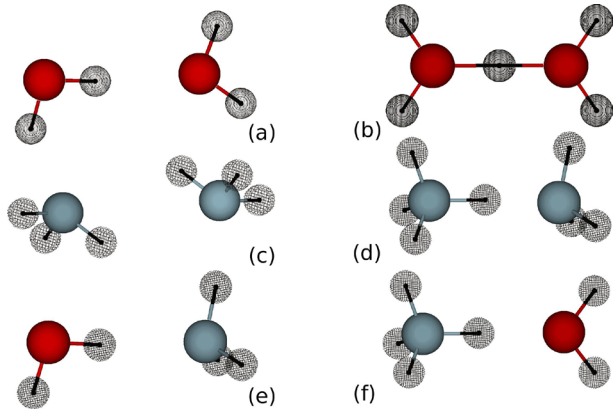

Figure 1. Schematic representation of hydrogen bonded dimers and complexes. (a)$[HOH\cdots OH_2]$ (b) $[H_2O\cdots H\cdots OH_2]^+$ (c)$[H_2NH\cdots NH_3]$ (d)$[H_3N\cdots H\cdots NH_3]^+$ (e)$[HOH\cdots NH_3]$ (f)$[H_3NH\cdots OH_2]^+$. Black grids represent hydrogen nuclei treated as quantum waves. Red and blue balls represent oxygen and nitrogen nuclei.

3 Computational details

The APMO/HF and APMO/MBPT(2) formalisms have been implemented in the LOWDIN program (Flores-Moreno et al., 2014; Reyes et al., 2019). A thorough examination of the APMO/HF/HPA equations shows that they arise as particular instances of the general APMO/HF expressions, obtained by omitting self-repulsion and self-exchange contributions. An analogous inspection of the APMO/MBPT(2)/HPA equations indicates that they correspond to the subset of APMO/MBPT(2) expressions in which the heavy particles are treated as distinguishable.

The object-oriented nature of LOWDIN allows APMO/HF/HPA and APMO/MBPT(2)/HPA calculations to be carried out directly. The user need only prepare an input file in which each heavy particle is defined as a distinguishable particle. For example, in a system with four quantum protons, each nucleus must be assigned a unique label, such as H_a, H_b, H_c, and H_d.

Conventional HF and MP2 electronic-structure calculations (hereafter denoted MO/HF and MO/MP2), as well as all APMO computations, were carried out using the LOWDIN program. In the APMO approach, hydrogen nuclei and negative muons were modeled in high-spin configurations (Reyes et al., 2005), whereas all other nuclei were represented as point charges. Self-consistent-field iterations were converged to 10^{-9} a.u. All calculations were run on an Intel Ultra 9 185H (4.800 GHz) with 64 GB RAM.

4 Results and Discussion

4.1 APMO/MBPT(2)/HPA energies

Total APMO/MBPT(2) and APMO/MBPT(2)/HPA energies for neutral and protonated water and ammonia hydrogen-bonded dimers (see Figure 1) were evaluated at MO/MP2-optimized geometries. Calculations employed the 6-31G(d,p) electronic basis set (Hehre et al., 1972) and the DZSPD nuclear basis set (Reyes et al., 2005; Webb et al., 2002). As summarized in Table 1, APMO/MBPT(2)/HPA total energies are at least 10^{-2} a.u. lower than their APMO/MBPT(2) counterparts. The table also reports zeroth-order and second-order correlation components. Zeroth-order energies (E_{APMO}), second-order electronic correlation ($E_{ee}^{(2)}$), and nuclear–nuclear correlation ($E_{nn}^{(2)}$) differ by less than 10^{-4} a.u. between

doi: https://doi.org/10.18257/raccefyn.3606

the two approaches. In contrast, nuclear–electron correlation energies ($E_{en}^{(2)}$) differ by about 10^{-2} a.u. and account for at least 99.8% of the total energy discrepancy.

The origin of the observed variations in nuclear–electron correlation energies can be rationalized by examining the APMO/MBPT(2) (Eq. 14) and APMO/MBPT(2)/HPA (Eq. 29) formulations. To this end, we derive the corresponding expressions for the hydrogen molecule employing the [STO-3G:DZS] electronic:nuclear basis sets (Hehre et al., 1969; Webb et al., 2002). In this system, two electrons occupy a single electronic orbital 1_e, and within this minimal electronic basis, there exists only one virtual orbital, 2_e. At the APMO/MBPT(2) level, the two protons are described by the nuclear orbitals 1_{H} and 2_{H} with two additional virtual nuclear orbitals, 3_{H} and 4_{H}. Within this theoretical approach, the proton–electron correlation energy contribution is given by

$$\begin{aligned} E_{en}^{(2)} = 2\frac{|\langle 1_e 1_{\mathrm{H}} \mid 2_e 3_{\mathrm{H}}\rangle|^2}{\varepsilon_{e1}+\varepsilon_{\mathrm{H}1}-\varepsilon_{e2}-\varepsilon_{\mathrm{H}3}} + 2\frac{|\langle 1_e 1_{\mathrm{H}} \mid 2_e 4_{\mathrm{H}}\rangle|^2}{\varepsilon_{e1}+\varepsilon_{\mathrm{H}1}-\varepsilon_{e2}-\varepsilon_{\mathrm{H}3}} + \\ 2\frac{|\langle 1_e 2_{\mathrm{H}} \mid 2_e 3_{\mathrm{H}}\rangle|^2}{\varepsilon_{e1}+\varepsilon_{\mathrm{H}2}-\varepsilon_{e2}-\varepsilon_{\mathrm{H}3}} + 2\frac{|\langle 1_e 2_{\mathrm{H}} \mid 2_e 4_{\mathrm{H}}\rangle|^2}{\varepsilon_{e1}+\varepsilon_{\mathrm{H}2}-\varepsilon_{e2}-\varepsilon_{\mathrm{H}4}}. \end{aligned} \tag{32}$$

Within the APMO/MBPT(2)/HPA approach, the two protons (H_a and H_b) are treated as distinguishable. Proton H_a occupies orbital 1_{H_a} and has a single virtual orbital 2_{H_a}, while proton H_b occupies orbital 1_{H_b} with one virtual orbital 2_{H_b}. At this level of theory, the proton–electron correlation energy is given by

$$E_{en}^{(2)} = 2\frac{|\langle 1_e 1_{H_a} \mid 2_e 2_{H_a}\rangle|^2}{\varepsilon_{e1}+\varepsilon_{H_a1}-\varepsilon_{e2}-\varepsilon_{H_a2}} + 2\frac{|\langle 1_e 1_{H_b} \mid 2_e 2_{H_b}\rangle|^2}{\varepsilon_{ea}+\varepsilon_{H_b1}-\varepsilon_{e2}-\varepsilon_{H_b2}}. \tag{33}$$

Equation 32 includes two more terms than Eq. 33, reflecting the larger number of possible excitations at the APMO/MBPT(2) level. The resulting nuclear–electron correlation energy is determined by the squared Coulomb integrals in the numerators and the eigenvalues of occupied and virtual electron and nuclear orbitals in the denominators. Table 2 lists the total APMO/MBPT(2) and APMO/MBPT(2)/HPA nuclear–electron correlation energies, together with the corresponding Coulomb integrals and orbital eigenvalues. At the APMO/MBPT(2) level, occupied nuclear orbitals have negative eigenvalues, and virtual nuclear orbitals have positive eigenvalues, whereas at the APMO/MBPT(2)/HPA level, both occupied and virtual nuclear orbitals exhibit negative eigenvalues. Using the eigenvalues presented in Table 2, the four denominators in Eq. 32 (APMO/MBPT(2) method) are equal to -5.0428 a.u., and the two denominators of Eq. 33 (APMO/MBPT(2)/HPA method) are equal to -1.3340 a.u.

We now examine the numerators in Eqs. 32 and 33. In the APMO/MBPT(2) expression (Eq. 32), the four denominators are identical, allowing us to factor them out and compute the numerator as the sum of the squared Coulomb integrals, yielding 2.750×10^{-3} a.u.^{2}. For the APMO/MBPT(2)/HPA expression (Eq. 33), factorization of the two energy terms and summation of the squared Coulomb integrals give 2.744×10^{-3} a.u.^{2} Because these numerators are essentially the same, any discrepancy in the nuclear–electron correlation energies arises from the denominators. As noted, the APMO/MBPT(2)/HPA denominator is nearly four times smaller than that in APMO/MBPT(2), leading to a nuclear–electron correlation energy that is correspondingly about four times larger in the APMO/MBPT(2)/HPA method.

The results obtained thus far demonstrate that differences in nuclear–electron correlation energies stem from variations in the eigenvalues of occupied and virtual orbitals. In most

Revista de la Academia Colombiana de Ciencias Exactas, Físicas y Naturales. 2026
doi: https://doi.org/10.18257/raccefyn.3606

Table 1. APMO/MBPT(2) and APMO/MBPT(2)/HPA total ($E_{MBPT(2)}$), zeroth-order (E_{APMO}) energies, electron-electron ($E^{(2)}_{ee}$), electronic-nuclear ($E^{(2)}_{en}$), nuclear ($E^{(2)}_{nn}$) correlation energies, in a.u., for hydrogen bonded dimers.

System	Reference	$E_{MBPT(2)}$	E_{APMO}	$(E^{(2)}_{ee})$	$(E^{(2)}_{en})$	$(E^{(2)}_{nn})$
[HOH · · ·OH2]	APMO/HF	-152.2973	-151.8878	-0.4011	-0.0085	-1 ×10^{-6}
	APMO/HF/HPA	-152.3082	-151.8878	-0.4011	-0.0194	-1 ×10^{-5}
[H2O · · ·H · · · OH2]$^{+}$	APMO/HF	-152.6109	-152.1949	-0.4058	-0.0102	-1 ×10^{-6}
	APMO/HF/HPA	-152.6232	-152.1949	-0.4058	-0.0225	-2 ×10^{-5}
[H2NH · · · NH3]	APMO/HF	-112.5402	-112.1391	-0.3880	-0.0130	-1 ×10^{-6}
	APMO/HF/HPA	-112.5582	-112.1391	-0.3880	-0.0311	-2 ×10^{-5}
[H3N · · ·H · · · NH 3]$^{+}$	APMO/HF	-112.9057	-112.4955	-0.3954	-0.0148	-2 ×10^{-6}
	APMO/HF/HPA	-112.9255	-112.4955	-0.3954	-0.0346	-3 ×10^{-5}
[HOH · · · NH3]	APMO/HF	-132.4238	-132.0179	-0.3952	-0.0107	-1 ×10^{-6}
	APMO/HF/HPA	-132.4382	-132.0179	-0.3952	-0.0251	-2 ×10^{-5}
[H3NH · · · OH2]$^{+}$	APMO/HF	-132.7700	-132.3593	-0.3982	-0.0125	-1 ×10^{-6}
	APMO/HF/HPA	-132.7863	-132.3593	-0.3982	-0.0288	-3 ×10^{-5}

Calculations were performed at the MO/MP2 6-31G(d,p) optimized geometries using the [6-31G(d,p):DZSPD] electronic:nuclear basis sets.

Table 2. APMO/MBPT(2) and APMO/MBPT(2)/HPA H_2 electronic and nuclear eigenvalues, integrals, and nuclear-electron correlation energies $(E^{(2)}_{en})$. Energies in a.u.

APMO/MBPT(2)		APMO/MBPT(2)/HPA	
ε_{e1}	-0.5603	ε_{e1}	-0.5603
ε_{e2}	0.7202	ε_{e2}	0.7202
$\varepsilon_{\mathrm{H}1}$	-1.0951	$\varepsilon_{\mathrm{H}_a1}$	-1.0951
$\varepsilon_{\mathrm{H}2}$	-1.0951	$\varepsilon_{\mathrm{H}_b1}$	-1.0951
$\varepsilon_{\mathrm{H}3}$	2.6672	$\varepsilon_{\mathrm{H}_a2}$	-1.0416
$\varepsilon_{\mathrm{H}4}$	2.6672	$\varepsilon_{\mathrm{H}_b2}$	-1.0416
$\langle 1_e 1_{\mathrm{H}} \mid 2_e 3_{\mathrm{H}} \rangle$	8.823×10^{-3}	$\langle 1_e 1_{\mathrm{H}_a} \mid 2_e 2_{\mathrm{H}_a} \rangle$	8.824×10^{-3}
$\langle 1_e 1_{\mathrm{H}} \mid 2_e 4_{\mathrm{H}} \rangle$	3.574×10^{-4}	$\langle 1_e 1_{\mathrm{H}_b} \mid 2_e 2_{\mathrm{H}_b} \rangle$	8.824×10^{-3}
$\langle 1_e 2_{\mathrm{H}} \mid 2_e 3_{\mathrm{H}} \rangle$	3.574×10^{-4}		
$\langle 1_e 2_{\mathrm{H}} \mid 2_e 4_{\mathrm{H}} \rangle$	8.823×10^{-3}		
$E^{(2)}_{en}$	-5.453×10^{-5}	$E^{(2)}_{en}$	-2.057×10^{-4}

Calculations were performed using the [STO-3G:DZS] electronic:nuclear basis sets at the MO/HF STO-3G optimized geometry.

cases, the APMO/HF and APMO/HF/HPA expressions yield identical eigenvalues for occupied (Eq. 8, Eq. 20) and virtual electronic orbitals (Eq. 9, Eq. 22). Likewise, the eigenvalues of occupied nuclear orbitals are effectively the same in APMO/HF and APMO/HF/HPA (Eq. 8, Eq. 21), since their only differences between them arise from the exchange terms, which are negligible (Reyes et al., 2005).

In contrast, the APMO/HF and APMO/HF/HPA expressions for the eigenvalues of virtual nuclear orbitals (Eq. 9 and Eq. 23) are not identical. At the APMO/HF level, Eq. 9 contains the sum of Coulomb integrals between a given virtual nuclear orbital and all occupied nuclear orbitals. In the APMO/HF/HPA approach, however, Eq. 23 omits the Coulomb interaction with the occupied nuclear orbital belonging to the same nuclear species (since APMO/HF/HPA treats each nucleus as a distinct species). Removing this repulsive contribution lowers the virtual nuclear eigenvalues in APMO/HF/HPA relative to APMO/HF.

doi: https://doi.org/10.18257/raccefyn.3606

Consequently, the occupied–virtual energy gaps are smaller in APMO/HF/HPA, leading to smaller denominators in the nuclear–electron correlation terms within APMO/MBPT(2)/HPA. If, as shown above, the sums of squared Coulomb integrals are comparable in both schemes, the nuclear–electron correlation energy from APMO/MBPT(2)/HPA will always be more stabilizing (more negative) than that obtained with APMO/MBPT(2).

The mechanism by which HPA increases correlation recovery is analogous to improved virtual orbital (IVO) techniques used in post-Hartree-Fock methods. The HPA reduces virtual orbital energies, leading to smaller energy denominators in the MBPT(2) expression, where smaller ε values result in smaller denominators and thus larger correlation corrections. This increases the amount of interspecies correlation recovered at the APMO/MBPT(2) level.

Distinct physical interpretations can be assigned to the nuclear virtual eigenvalues obtained with the APMO/HF and APMO/HF/HPA approaches. Within APMO/HF, a nuclear virtual eigenvalue can be interpreted as the nuclear affinity of the molecule, in direct analogy to the connection between an electronic virtual eigenvalue and the electronic affinity (Pedraza-González et al., 2016; Romero et al., 2012; Szabo & Ostlund, 1996). In contrast, within APMO/HF/HPA, a nuclear virtual eigenvalue corresponds to the nuclear ionization potential.

Swalina et al. (2005) investigated an analogous eigenvalue difference for a single active proton within an alternative MBPT(2) treatment of proton–electron correlation. By the same reasoning, the energy gaps in the APMO/MBPT(2) and APMO/MBPT(2)/HPA nuclear–nuclear correlation contributions can be interpreted.

To quantify the effect of the nuclear–electron correlation recovered via the HPA, Table 3 reports APMO/MBPT(2) and APMO/MBPT(2)/HPA total energies and nuclear–electron correlation energies for the H_2 isotopologues, together with the MCMO full-CI data of Ishimoto, Tachikawa, and Nagashima (2008). All calculations, carried out both with and without the TRF correction, employed a 5s2p1d electronic (Dunning, 1989) and a 5s5p5d nuclear (Nakai, 2002) basis set.

APMO/MBPT(2)/HPA results agree more closely with full-CI values than those from APMO/MBPT(2), indicating that APMO/MBPT(2)/HPA should recover more nuclear-electron correlation. However, this approach recovers only about 45% of the full-CI nuclear–electron correlation energy without the TRF correction and about 35% with it, which may be insufficient for applications requiring highly detailed physical descriptions. These larger corrections partially compensate for the incomplete treatment of interspecies correlation, in a similar fashion as improved virtual orbital schemes for post-HF methods. However, this compensation is system-dependent and not systematic.

4.2 APMO/MBPT(2)/HPA computational efficiency

We carried out APMO/MBPT(2) and APMO/MBPT(2)/HPA single-point computations on linear hydrogen fluoride chains $(HF)_n$ with $n = 1$–20. A schematic of these systems is shown in Figure 2. All calculations employed the [6-31:DZSP] electronic:nuclear basis set (Hehre et al., 1972; Webb et al., 2002), selected because it yields a comparable number of contractions per HF unit.

Our results show that total computation times with the APMO/MBPT(2)/HPA scheme are consistently shorter. To understand why APMO/MBPT(2)/HPA is faster than plain APMO/MBPT(2), we examined how the HPA affects the four-center integral transformation, which constitutes the most demanding part of MBPT(2) calculations. We restrict our analysis to nuclear–electron and nuclear–nuclear transformations, since electron–electron transformation times are the same for both approaches. As illustrated in Figure 3, introducing the HPA substantially lowers the required transformation time in each case and also improves the scaling of these transformations with the number of HF molecules.

Revista de la Academia Colombiana de Ciencias Exactas, Físicas y Naturales. 2026
doi: https://doi.org/10.18257/raccefyn.3606

Table 3. APMO/MBPT(2), APMO/MBPT(2)/HPA, TRF-APMO/MBPT(2), TRF-APMO/MBPT(2)/HPA and MCMO full-CI[b] total (E) and nuclear-electron correlation energies (E_{en}) for the H_2, HD, and D_2 molecules. Energies in a.u.[a]

System	Method	APMO		TRF-APMO	
		E	E_{en}	E	E_{en}
H_2	MBPT(2)	-1.0952	-0.0119	-1.1379	-0.0022
	MBPT(2)/HPA	-1.1102	-0.0254	-1.1425	-0.0066
	MCMO/full-CI[b]	-1.1393	-0.0539	-1.1576	-0.0194
HD	MBPT(2)	-1.1043	-0.0098	-1.1415	-0.0020
	MBPT(2)/HPA	-1.1173	-0.0217	-1.1456	-0.0058
	MCMO/full-CI[b]	-1.1436	-0.0464	-1.1596	-0.0179
D_2	MBPT(2)	-1.1134	-0.0078	-1.1456	-0.0014
	MBPT(2)/HPA	-1.1246	-0.0180	-1.1490	-0.0047
	MCMO/full-CI[b]	-1.1482	-0.0412	-1.1614	-0.0137

[a] MBPT(2) calculations were performed using the [5s2p1d:5s5p5d] electronic:nuclear basis sets at the APMO/MBPT(2)/HPA optimized geometry; [b] Ref. (Ishimoto, Tachikawa, & Nagashima, 2008) Full-CI MCMO calculations with a [5s2p1d:1s1p1d] electronic:nuclear basis set

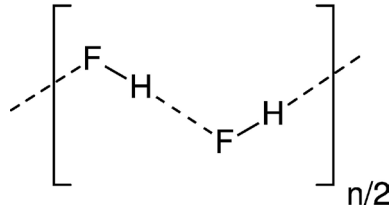

Figure 2. Schematic representation of hydrogen fluoride chains. Hydrogen nuclei were treated as quantum waves

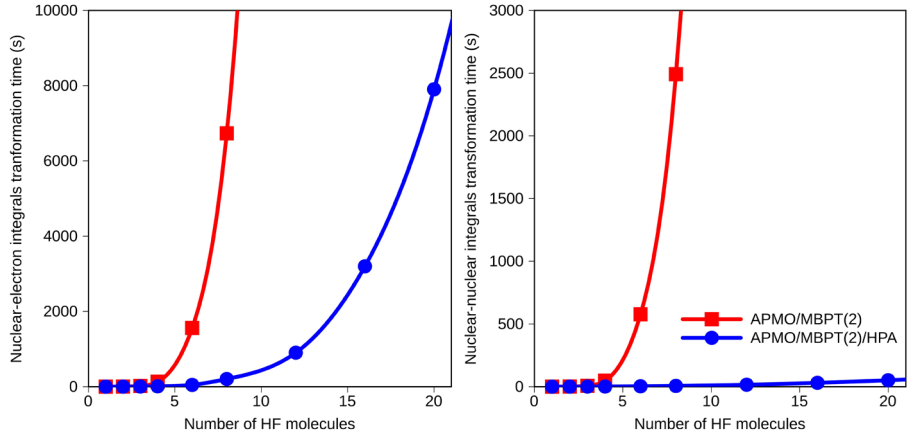

Figure 3. Nuclear-electron (right) and nuclear-nuclear (left) integral transformation times for HF chains of different lengths. Continuous lines represent cubic spline interpolations.

To clarify the origin of the reduced scaling, we examine the number of integrals needed to compute the correlation energies in Eqs. 14, 28, and 29 for both approaches. The number of integrals required for the APMO/MBPT(2) nuclear–electron correlation energy scales as $N_e N_H (B_e - N_e)(B_H - N_H)$, where N_e and N_H denote the numbers of occupied electronic and nuclear orbitals, and B_e and B_H denote the sizes of the electronic and nuclear basis sets, respectively. The corresponding count for the nuclear–nuclear correlation energy scales as

$N_H{}^2(B_H - N_H)^2$. In this scheme, N_e, N_H, B_e, and B_H all grow linearly with the length of the HF chain, so the overall number of integrals in APMO/MBPT(2) exhibits quartic scaling with system size. Owing to the stepwise atomic-to-molecular integral transformation algorithm (Yamamoto & Nagashima, 2005), the nuclear–nuclear and nuclear–electron integral transformations display a formal quintic scaling with respect to system size.

The number of integrals required to obtain the APMO/MBPT(2)/HPA nuclear-electron correlation energy is proportional to $N_nN_e(B_H - 1)(B_e - N_e)$, where N_n is the number of protons in the system. The number of integrals required to obtain the APMO/MBPT(2)/HPA nuclear-nuclear correlation energy is proportional to $N_n{}^2(B_H - 1)^2$. The use of HPA and localized basis sets has two consequences: the number of nuclear occupied orbitals is always one, and the basis set size for each nucleus, B_H, is independent of the system size. Therefore, only N_n,N_e and B_e increase with the size of the HF chain. Consequently, the number of integrals required by the APMO/MBPT(2)/HPA nuclear-electron and nuclear-nuclear correlation energies increases cubically and quadratically, respectively. Using the stepwise integral transformation algorithm (Yamamoto & Nagashima, 2005), the formal scaling of the APMO/MBPT(2)/HPA nuclear-electron and nuclear-nuclear integral transformations is quartic and cubic, respectively. As illustrated in Figure 4, the standard APMO/MBPT(2) method exhibits $O(N^6)$ scaling, whereas APMO/MBPT(2)/HPA lowers this to $O(N^5)$ by decoupling the heavy-particle degrees of freedom. An examination of the timing data from our computations confirms that the observed scaling behavior agrees with the theoretical expectations.

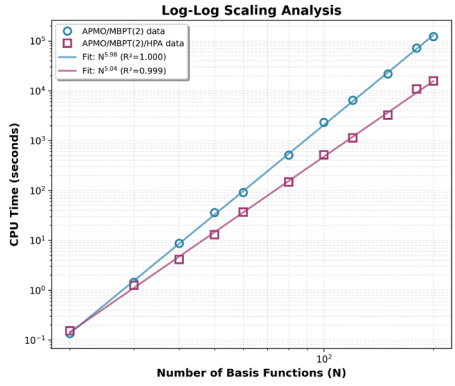

Figure 4. Analysis of computational time versus basis set size.

4.3 Negative muon-electron correlation

We have previously examined the electronic structure of atoms and molecules containing negative muons using the APMO/HF methodology (Moncada, Cruz, & Reyes, 2013b; Moncada et al., 2012; Posada et al., 2014). Those studies indicated that an atom containing a single negative muon (μ) effectively behaves like an all-electron atom with nuclear charge $Z - 1$, because the muon density is strongly localized at the nucleus and screens one unit of its positive charge. In the earlier work, however, muon–electron correlation was neglected. To assess its impact within the APMO approach, we now report APMO/MBPT(2) and APMO/MBPT(2)/HPA calculations for muonic helium, Heμ, muonic lithium, Liμ, and the muonic helium dimer, $(\mathrm{He}\mu)_2$. These computations employ large even-tempered basis sets (Moncada et al., 2012; Posada et al., 2014) for both the negative muon and the electrons and are provided in the Supporting Information. For simplicity, all nuclei are modeled as infinitely massive point charges.

Revista de la Academia Colombiana de Ciencias Exactas, Físicas y Naturales. 2026
doi: https://doi.org/10.18257/raccefyn.3606

As shown in Table 4, the muon–electron correlation energy depends strongly on the selected basis set. Adding 5p functions to a 10s basis enhances this correlation energy by three orders of magnitude, and expanding the basis further from 10s5p to 20s10p yields an additional increase of one order of magnitude. However, increasing the number of s and p functions beyond this, or adding d functions, does not lead to any further gain in muon–electron correlation. The largest (negative) correlation energy obtained was -1.70×10^{-6} a.u. for the muonic helium dimer with the 31s13p basis, a value that can generally be regarded as negligible for most chemical applications.

Examination of the muon–electron correlation energy shows that the APMO/MBPT(2)/HPA approach retrieves a larger portion of the correlation energy than APMO/MBPT(2). This discrepancy arises from the same effect identified for nuclear–electron correlation: the APMO/HF/HPA muonic virtual eigenvalues lack the muon–muon repulsive contribution present in the APMO/HF eigenvalues.

To assess the reliability of these results, we carried out a two-particle full-CI calculation for the muonic helium atom using a 20s10p basis set. This yielded a muon–electron correlation energy of -0.596×10^{-6} a.u., in good agreement with the APMO/MBPT(2)/HPA value of -0.590×10^{-6} a.u.

These findings contrast with the previously examined nuclear–electron correlation: in systems containing negative muons and electrons, the APMO/HF reference accurately captures the electron–muon interaction because muon–electron correlation is essentially negligible. This enables the use of APMO/HF for the negative muon–electron part in combination with highly correlated electronic-structure methods to compute very precise chemical properties of muonic atoms and molecules (Aguirre et al., 2013).

Table 4. APMO/MBPT(2) and APMO/MBPT(2)/HPA total (EMBPT(2)), electron correlation ($E^{(2)}_{ee}$) and negative muon-electron correlation ($E^{(2)}_{e\mu}$) energies for muonic helium, muonic lithium, and muonic helium dimer. Energies in a.u.[a]

		APMO/MBPT(2)			APMO/MBPT(2)/HPA		
System	[e−:μ−] basis sets	$E_{MBPT(2)}$	$(E^{(2)}_{ee})$	$(E^{(2)}_{e\mu})/10^{-6}$	$E_{MBPT(2)}$	$(E^{(2)}_{ee})$	$(E^{(2)}_{e\mu})/10^{-6}$
$^{\infty}$Heμ	[10s : 10s]	-413.9248		-0.0002	-413.9248		-0.0002
	[10s5p : 10s5p]	-413.9248		-0.0337	-413.9248		-0.0464
	[20s10p : 20s10p]	-414.0107		-0.4557	-414.0107		-0.5905
	[20s10p5d : 20s10p5d]	-414.0357		-0.4557	-414.0357		-0.5904
	[31s13p : 31s13p]	-414.0366		-0.4629	-414.0366		-0.5976
$^{\infty}$Liμ	[10s : 10s]	-932.5036	-0.0134	-0.0002	-932.5036	-0.0134	-0.0002
	[10s5p : 10s5p]	-932.5200	-0.0298	-0.0342	-932.5200	-0.0298	-0.0427
	[20s10p : 20s10p]	-933.1740	-0.0324	-0.9494	-933.1740	-0.0324	-1.1563
	[20s10p5d : 20s10p5d]	-933.3479	-0.0348	-0.9489	-933.3479	-0.0348	-1.1556
	[31s13p : 31s13p]	-933.3513	-0.0324	-0.9799	-933.3513	-0.0324	-1.1867
$(^{\infty}$He$\mu)_2$	[10s : 10s]	-827.9966	-0.0185	-0.0005	-827.9966	-0.0185	-0.0006
	[10s5p : 10s5p]	-828.0135	-0.0304	-0.1040	-828.0135	-0.0304	-0.1428
	[20s10p : 20s10p]	-828.1856	-0.0307	-1.2978	-828.1856	-0.0307	-1.6788
	[20s10p5d : 20s10p5d]	-828.2375	-0.0324	-1.2990	-828.2375	-0.0324	-1.6804
	[31s13p : 31s13p]	-828.2374	-0.0307	-1.3179	-828.2374	-0.0307	-1.6988

$(^{\infty}$He$\mu)_2$ was calculated at an internuclear separation of 0.7414 . For this system, muon-muon correlation is lower than 10^{-13} a.u.

5 Concluding remarks

We present a modified second-order many-body perturbation theory tailored to the Any Particle Molecular Orbital method. Here, the reference state is built as a product of Slater determinants for the light particles (electrons) and Hartree products of localized nuclear orbitals for the heavy particles (muons, nuclei). Studies on hydrogen-bonded dimers and the hydrogen molecule demonstrate that the Hartree product approximation (HPA) affects the MBPT(2) energies. Decomposition of the correlation energy indicates that the HPA enhances the fraction of nuclear–electron correlation captured by MBPT(2). Applications to hydrogen fluoride chains of varying lengths further show that the HPA lowers the computational cost of MBPT(2) by reducing the formal scaling of the nuclear–electron and nuclear–nuclear integral transformations.

Using the APMO/MBPT(2) approach for muonic helium, muonic lithium, and the muonic helium dimer shows that muon–electron correlation is only about 1×10^{-6} a.u., and thus can be safely ignored when examining the chemistry of muonic atoms.

It should be emphasized that MBPT(2) constitutes only an initial approximation to incorporating interspecies correlation within APMO calculations. Under the HPA, its performance varies markedly: for certain systems, such as the H_2 isotopologues, it recovers only about 45% of the full-CI interspecies correlation energy, whereas for others, such as muonic helium, it reaches approximately 99%. This description could be systematically improved by extending the APMO approach to explicitly correlated wave-function methods (Cafiero et al., 2003; Hoshino et al., 2011), multicomponent density functional theory (Kreibich & Gross, 2001), or multiconfigurational strategies (Ishimoto, Tachikawa, & Nagashima, 2008). However, the computational demands of these approaches are typically prohibitive, restricting their use to small systems. Consequently, the APMO/MBPT(2)/HPA scheme provides a pragmatic and efficient entry point for investigating interspecies correlation effects in systems of medium size. This paves the way for examining H/D isotope effects, with potential use in isotope separation methods, as well as for studying muonic molecules in the context of muon spin spectroscopy. The method is intended primarily for exploratory work and for qualitative or semi-quantitative analyses, rather than for fully quantitative predictions. HPA should be used for initial exploratory studies and subsequently validated with higher-level approaches such as CCSD(T).

6 Acknowledgements

We are grateful to Dr. Felix Moncada for his valuable insights. We acknowledge the support of UNAL (HERMES project 63579).

Authors contribution

The author of this work solely conceived the idea, developed the theory, performed the calculations and analysis, and wrote the manuscript.

Conflict of interests

The author declares no conflict of interest.

References

Aguirre, N. F., Villarreal, P., Delgado-Barrio, G., Posada, E., Reyes, A., Biczysko, M., Mitrushchenkov, A., & de Lara-Castells, M. (2013). Including nuclear quantum effects into highly correlated electronic structure calculations of weakly bound systems. *The Journal of Chemical Physics*, *138*(18), 184113. https://doi.org/10.1063/1.4803546

doi: https://doi.org/10.18257/raccefyn.3606

Auer, B., & Hammes-Schiffer, S. (2010). Localized Hartree product treatment of multiple protons in the nuclear-electronic orbital framework. *The Journal of Chemical Physics*, *132*(8), 084110. https://doi.org/10.1063/1.3323015

Born, M., & Oppenheimer, J. R. (1927). Zur Quantentheorie der Molekeln. *Annalen der Physik*, *84*(20), 457–484. https://doi.org/10.1002/andp.19273892002

Cafiero, M., Bubin, S., & Adamowicz, L. (2003). Non-Born–Oppenheimer calculations of atoms and molecules. *Physical Chemistry Chemical Physics*, *5*(7), 1491–1501. https://doi.org/10.1039/B211422M

Charry, J., Varella, M. T. d. N., & Reyes, A. (2018). Binding matter with antimatter: The covalent positron bond. *Angewandte Chemie International Edition*, *130*(29), 8997–9002. https://doi.org/10.1002/anie.201804538

Charry Martinez, J. A., Barborini, M., & Tkatchenko, A. (2022). Correlated wave functions for electron-positron interactions in atoms and molecules. *Journal of Chemical Theory and Computation*, *18*(4), 2267–2280. https://doi.org/10.1021/acs.jctc.1c01211

Dunning, J., Thom H. (1989). Gaussian basis sets for use in correlated molecular calculations. I. The atoms boron through neon and hydrogen. *The Journal of Chemical Physics*, *90*(2), 1007–1023. https://doi.org/10.1063/1.456153

Flores-Moreno, R., Posada, E., Moncada, F., Romero, J., Charry, J., Díaz-Tinoco, M., González, S. A., Aguirre, N. F., & Reyes, A. (2014). LOWDIN: The any particle molecular orbital code. *International Journal of Quantum Chemistry*, *114*(1), 50–56. https://doi.org/10.1002/qua.24531

Fowler, D., & Brorsen, K. R. (2022). (T) correction for multicomponent coupled-cluster theory for a single quantum proton. *Journal of Chemical Theory and Computation*, *18*(12), 7298–7305. https://doi.org/10.1021/acs.jctc.2c00701

González, S. A., Aguirre, N. F., & Reyes, A. (2008). Theoretical investigation of isotope effects: The any-particle molecular orbital code. *International Journal of Quantum Chemistry*, *108*(10), 1742–1749. https://doi.org/10.1002/qua.21728

González, S. A., & Reyes, A. (2010). Nuclear quantum effects on the He_2H^+ complex with the nuclear molecular orbital approach. *International Journal of Quantum Chemistry*, *110*(4), 689–696. https://doi.org/10.1002/qua.22055

Hehre, W. J., Ditchfield, R., & Pople, J. A. (1972). Self—Consistent Molecular Orbital Methods. XII. Further Extensions of Gaussian—Type Basis Sets for Use in Molecular Orbital Studies of Organic Molecules. *The Journal of Chemical Physics*, *56*(6), 2257–2261. https://doi.org/10.1063/1.1677527

Hehre, W. J., Stewart, R. F., & Pople, J. A. (1969). Self-Consistent Molecular-Orbital Methods. I. Use of Gaussian Expansions of Slater-Type Atomic Orbitals. *The Journal of Chemical Physics*, *51*(6), 2657–2664. https://doi.org/10.1063/1.1672392

Hoshino, M., & Nakai, H. (2006). Elimination of translational and rotational motions in nuclear orbital plus molecular orbital theory: Application of Møller-Plesset perturbation theory. *The Journal of Chemical Physics*, *124*(19), 194110. https://doi.org/10.1063/1.2193513

Hoshino, M., Tsukamoto, Y., & Nakai, H. (2007). Development of analytic energy gradient method in nuclear orbital plus molecular orbital theory. *International Journal of Quantum Chemistry*, *107*(14), 2575–2585. https://doi.org/10.1002/qua.21456

Hoshino, M., Nishizawa, H., & Nakai, H. (2011). Rigorous non-born-oppenheimer theory: Combination of explicitly correlated Gaussian method and nuclear orbital plus molecular orbital theory. *The Journal of Chemical Physics*, *135*(2), 024111. https://doi.org/10.1063/1.3609344

Ishii, Y., Kuwahata, K., Shimazaki, T., & Tachikawa, M. (2025). Theoretical analysis of H/D isotope effect in $K_3H(SO_4)_2$ and its influence on phase transition temperature. *Physical Chemistry Chemical Physics*, *28*. https://doi.org/10.1039/D5CP02885J

Ishimoto, T., Ishihara, Y., Teramae, H., Baba, M., & Nagashima, U. (2008). H/D isotope effect of methyl internal rotation for acetaldehyde in ground state as calculated from a multicomponent molecular orbital method. *The Journal of Chemical Physics*, *128*(18), 184309. https://doi.org/10.1063/1.2913164

Ishimoto, T., Tachikawa, M., & Nagashima, U. (2006). Electron-electron and electron-nucleus correlation effects on exponent values of Gaussian-type functions for quantum protons and deuterons. *The Journal of Chemical Physics*, *125*(4), 044103. https://doi.org/10.1063/1.2222378

Ishimoto, T., Tachikawa, M., & Nagashima, U. (2008). Simultaneous analytical optimization of variational parameters in Gaussian-type functions with full configuration interaction of multicomponent molecular orbital method by elimination of translational and rotational motions: Application to isotopomers of the hydrogen molecule. *The Journal of Chemical Physics*, *128*(16), 164118. https://doi.org/10.1063/1.2902973

Ishimoto, T., Tachikawa, M., & Nagashima, U. (2009). Review of multicomponent molecular orbital method for direct treatment of nuclear quantum effect. *International Journal of Quantum Chemistry*, *109*(12), 2677–2694. https://doi.org/10.1002/qua.22069

Kaneko, M., Udagawa, T., & Tachikawa, M. (2010). Geometric isotope effect on low barrier hydrogen-bonding systems of acetic acid dimer, formic acid dimer, and their anionic clusters by using the multi-component molecular orbital method. *Journal of Computer Chemistry, Japan*, *9*(1), 21–28. https://doi.org/10.2477/jccj.H2113

Kikuta, Y., Ishimoto, T., & Nagashima, U. (2008). Geometrical and kinetic isotope effects on R–H (D)$\cdots$R type intramolecular hydrogen bonds (R= CH_2, NH, and O) using a multi-component molecular orbital method. *Bulletin of the Chemical Society of Japan*, *81*(7), 820–825. https://doi.org/10.1246/bcsj.81.820

Kita, Y., & Tachikawa, M. (2009). Nuclear quantum effects on molecular magnetic properties. *Journal of Molecular Structure: THEOCHEM*, *912*(1-3), 2–4. https://doi.org/10.1016/j.theochem.2009.04.032

Kreibich, T., & Gross, E. K. U. (2001). Multicomponent density-functional theory for electrons and nuclei. *Physical Review Letters*, *86*(14), 2984–2987. https://doi.org/10.1103/PhysRevLett.86.2984

Moncada, F., Cruz, D., & Reyes, A. (2012). Muonic alchemy: Transmuting elements with the inclusion of negative muons. *Chemical Physics Letters*, *539-540*, 209–213. https://doi.org/10.1016/j.cplett.2012.03.073

Moncada, F., Cruz, D., & Reyes, A. (2013a). Electronic properties of atoms and molecules containing one and two negative muons. *Chemical Physics Letters*, *570*, 16–21. https://doi.org/10.1016/j.cplett.2013.03.047

Moncada, F., Cruz, D., & Reyes, A. (2013b). Electronic properties of atoms and molecules containing one and two negative muons. *Chemical Physics Letters*, *570*, 16–21. https://doi.org/10.1016/j.cplett.2013.03.047

Moncada, F., González, S. A., & Reyes, A. (2010). First principles investigation of hydrogen isotope effects in $[XSO_4–H–SO_4X]^-$ (X = H, K) complexes. *Molecular Physics*, *108*(12), 1545–1552. https://doi.org/10.1080/00268971003716616

Moncada, F., Uribe, L. S., Romero, J., & Reyes, A. (2013a). Hydrogen isotope effects on covalent and noncovalent interactions: The case of protonated rare gas clusters. *International Journal of Quantum Chemistry*, *113*(22), 1556–1561. https://doi.org/10.1002/qua.24479

Moncada, F., Uribe, L. S., Romero, J., & Reyes, A. (2013b). Hydrogen isotope effects on covalent and noncovalent interactions: The case of protonated rare gas clusters. *International Journal of Quantum Chemistry*, *113*(10), 1556–1561. https://doi.org/10.1002/qua.24357

Moreno, D. V., González, S. A., & Reyes, A. (2010). Secondary hydrogen isotope effects on the structure and stability of cation-π complexes (Cation = Li^+, Na^+, K^+ and π = Acetylene, Ethylene, Benzene). *The Journal of Physical Chemistry A*, *114*(36), 9231–9236. https://doi.org/10.1021/jp1038237

Moreno, D. V., González, S. A., & Reyes, A. (2011). Turning symmetric an asymmetric hydrogen bond with the inclusion of nuclear quantum effects: The case of the $[CN\cdots H\cdots NC]^-$-complex. *The Journal of Chemical Physics*, *134*(2), 024115. https://doi.org/10.1063/1.3523961

Nakai, H. (2002). Simultaneous determination of nuclear and electronic wave functions without Born–Oppenheimer approximation: Ab initio NO^+ MO/HF theory. *International Journal of Quantum Chemistry*, *86*(6), 511–517. https://doi.org/10.1002/qua.10026

Nakai, H. (2007). Nuclear orbital plus molecular orbital theory: Simultaneous determination of nuclear and electronic wave functions without Born–Oppenheimer approximation. *International Journal of Quantum Chemistry*, *107*(15), 2849–2869. https://doi.org/10.1002/qua.21457

Nakai, H., Ikabata, Y., Tsukamoto, Y., Imamura, Y., Miyamoto, K., & Hoshino, M. (2007). Isotope effect in dihydrogen-bonded systems: Application of the analytical energy gradient method in the nuclear orbital plus molecular orbital theory. *Molecular Physics*, *105*(20-22), 2649–2657. https://doi.org/10.1080/00268970701648713

Nakai, H., & Sodeyama, K. (2003). Many-body effects in nonadiabatic molecular theory for simultaneous determination of nuclear and electronic wave functions: Ab initio NOMO-MBPT and CC methods. *The Journal of Chemical Physics*, *118*(3), 1119. https://doi.org/10.1063/1.1528951

Nakai, H., Hoshino, M., Miyamoto, K., & Hyodo, S. (2005). Elimination of translational and rotational motions in nuclear orbital plus molecular orbital theory. *The Journal of Chemical Physics*, *122*(16), 164101. https://doi.org/10.1063/1.1884601

Pavošević, F., Culpitt, T., & Hammes-Schiffer, S. (2019). Multicomponent coupled cluster singles and doubles theory within the nuclear-electronic orbital framework. *Journal of Chemical Theory and Computation*, *15*(1), 338–347. https://doi.org/10.1021/acs.jctc.8b00975

Pedraza-González, L., Romero, J., Alí-Torres, J., & Reyes, A. (2016). Prediction of proton affinities of organic molecules using the any-particle molecular-orbital second-order proton propagator approach. *Physical Chemistry Chemical Physics*, *18*(39), 27185–27189. https://doi.org/10.1039/C6CP13455F

Peng, Q., Zhang, X., Hung, L., Carter, E. A., & Lu, G. (2008). Quantum simulation of materials at micron scales and beyond. *Physical Review B*, *78*(5), 054118. https://doi.org/10.1103/PhysRevB.78.054118

Posada, E., Moncada, F., & Reyes, A. (2014). Negative muon chemistry: The quantum muon effect and the finite nuclear mass effect. *The Journal of Physical Chemistry A*, *118*(40), 9491–9499. https://doi.org/10.1021/jp505852b

Reyes, A., Pak, M. V., & Hammes-Schiffer, S. (2005). Investigation of isotope effects with the nuclear-electronic orbital approach. *The Journal of Chemical Physics*, *123*(6), 064104. https://doi.org/10.1063/1.1990116

Reyes, A., Moncada, F., & Charry, J. (2019). The any particle molecular orbital approach: A short review of the theory and applications. *International Journal of Quantum Chemistry*, *119*(2), e25705. https://doi.org/10.1002/qua.25705

Romero, J., Posada, E., Flores-Moreno, R., & Reyes, A. (2012). A generalized any particle propagator theory: Assessment of nuclear quantum effects on electron propagator calculations. *The Journal of Chemical Physics*, *137*(7), 074105. https://doi.org/10.1063/1.4742869

Stanke, M., Kedziorski, A., & Adamowicz, L. (2026). High-accuracy non-Born-Oppenheimer calculations with all-electron explicitly correlated Gaussians of finite-nuclear-mass effects in the spectrum of the ten lowest ^1D Rydberg states of beryllium. *Physical Review A*, *113*(1), 012814. https://doi.org/10.1103/PhysRevA.113.012814

Swalina, C., Pak, M. V., & Hammes-Schiffer, S. (2005). Alternative formulation of many-body perturbation theory for electron-proton correlation. *Chemical Physics Letters*, *404*(4-6), 394–399. https://doi.org/10.1016/j.cplett.2005.01.114

Szabo, A., & Ostlund, N. S. (1996). *Modern quantum chemistry: Introduction to Advanced Electronic Structure Theory*. Dover Publications.

Tachikawa, M. (2002). Multi-component molecular orbital theory for electrons and nuclei including many-body effect with full configuration interaction treatment: Isotope effects on hydrogen molecules. *Chemical Physics Letters*, *360*(5-6), 494–500. https://doi.org/10.1016/S0009-2614(02)00881-3

Tachikawa, M. (2008). Multi-component first-principles calculation on isotope effect in hydrogen-bonded dieletric materials $K_3H(SO_4)_2$ and $K_3D(SO_4)_2$. *Integrated Ferroelectrics*, *100*(1), 72–78. https://doi.org/10.1080/10584580802540549

Tachikawa, M., Ishimoto, T., Tokiwa, H., Kasatani, H., & Deguchi, K. (2002). First-principle calculation on isotope effect in KH_2PO_4 and KD_2PO_4 of hydrogen-bonded dielectric materials. Approach with dynamic extended molecular orbital method. *Ferroelectrics*, *268*(1), 3–9. https://doi.org/10.1080/00150190211440

Tachikawa, M., Mori, K., Nakai, H., & Iguchi, K. (1998). An extension of ab initio molecular orbital theory to nuclear motion. *Chemical Physics Letters*, *290*(4-5), 437–442. https://doi.org/10.1016/S0009-2614(98)00519-5

Tachikawa, M., & Osamura, Y. (2000). Simultaneous optimization of exponents, centers of Gaussian-type basis functions, and geometry with full-configuration interaction wave function: Application to the ground and excited states of hydrogen molecule. *The Journal of Chemical Physics*, *113*(11), 4942–4947. https://doi.org/10.1063/1.1290432

Tanaka, H., Kuwahata, K., Tachikawa, M., & Udagawa, T. (2025). Nuclear quantum and H/D isotope effects on hydrogen-bond symmetrization in lithium hydroxide crystals at high pressure. *The Journal of Chemical Physics*, *163*. https://doi.org/10.1063/5.0276067

Udagawa, T., Ishimoto, T., Tokiwa, H., Tachikawa, M., & Nagashima, U. (2006). Geometric isotope effect of various intermolecular and intramolecular C-H$\cdots$O hydrogen bonds, using the multicomponent molecular orbital method. *The Journal of Physical Chemistry A*, *110*(23), 7279–7285. https://doi.org/10.1021/jp0605953

Udagawa, T., & Tachikawa, M. (2006). H/D isotope effect on porphine and porphycene molecules with multicomponent hybrid density functional theory. *The Journal of Chemical Physics*, *125*(24), 244105. https://doi.org/10.1063/1.2403855

Udagawa, T., & Tachikawa, M. (2009). *Multi-component molecular orbital theory*. Nova Science Publishers.

Webb, S. P., Iordanov, T., & Hammes-Schiffer, S. (2002). Multiconfigurational nuclear-electronic orbital approach: Incorporation of nuclear quantum effects in electronic structure calculations. *The Journal of Chemical Physics*, *117*(9), 4106–4115. https://doi.org/10.1063/1.1494985

Yamamoto, S., & Nagashima, U. (2005). Four-index integral transformation exploiting symmetry. *Computer Physics Communications*, *166*(1), 58–65. https://doi.org/10.1016/j.cpc.2004.10.003

Yodsin, N., Udagawa, T., Daengngern, R., Jungsutthiwong, S., & Tachikawa, M. (2025). Unraveling H_2 dissociation in CO_2 hydrogenation on frustrated Lewis pair-functionalized UiO–67: DFT and nuclear quantum effects. *International Journal of Hydrogen Energy*, *195*, 152499. https://doi.org/10.1016/j.ijhydene.2025.152499